


Nonperturbative Decoupling of Massive Fermions

Tobias Rindlisbacher^{✉*}

Albert Einstein Center for Fundamental Physics and Institute for Theoretical Physics, University of Bern,
Sidlerstrasse 5, CH-3012 Bern, Switzerland

Kari Rummukainen^{✉,†}, Ahmed Salami^{✉,‡} and Kimmo Tuominen^{✉,§}

Department of Physics and Helsinki Institute of Physics, P.O. Box 64, FI-00014 University of Helsinki, Finland

 (Received 23 November 2021; revised 2 April 2022; accepted 29 August 2022; published 23 September 2022)

SU(2) gauge theory with $N_f = 24$ massless fermions is noninteracting at long distances, i.e., it has an infrared fixed point at vanishing coupling. With massive fermions, the fermions are expected to decouple at energy scales below the fermion mass, and the infrared behavior is that of confining SU(2) pure gauge theory. We demonstrate this behavior nonperturbatively with lattice Monte Carlo simulations by measuring the gradient flow running coupling.

DOI: [10.1103/PhysRevLett.129.131601](https://doi.org/10.1103/PhysRevLett.129.131601)

Introduction.—Non-Abelian gauge field theories are at the core of the standard model of particle physics, as well as many of its extensions. The behavior of these theories is largely dictated by their fermionic matter content. Because of their applications in beyond standard model scenarios, asymptotically-free theories with an infrared fixed point [1–4] have recently attracted attention. On the lattice, the properties of these types of theories have been studied for SU(2) gauge theory with matter fields in the fundamental [5–9] or adjoint [10–18] representation.

Much less is known about the dynamics of theories that are not asymptotically-free, i.e., where the coupling constant does not vanish at high energies. For SU(N) gauge theory with fundamental representation Dirac fermions this happens when the number of fermions N_f is larger than $11N/2$. While these theories are not directly relevant for the standard model, they pose a challenge for our understanding of the gauge field dynamics and the applicability of lattice computation methods.

More concretely, let us consider the evolution of the coupling constant in SU(2) gauge theory with $N_f = 24$ Dirac fermions. If fermions are massless, the theory is noninteracting at long distances, i.e., it has an infrared (IR) fixed point at vanishing coupling [19,20]. At shorter distances (high energy) the coupling is expected to grow until it diverges at an ultraviolet (UV) Landau pole. This conclusion is supported by our earlier study of the evolution of the coupling with massless fermions [21].

A nonvanishing fermion mass m introduces an additional scale to the system. While the UV properties remain to a large extent unaffected by this, the IR physics changes dramatically: fermions are expected to decouple at energy scales $\mu \ll m$ (distance scales $\lambda \gg 1/m$), and the theory behaves like a confining pure gauge SU(2) theory with coupling that grows in the infrared. Thus, the expectation is that the coupling constant has a minimum near energy scale $\mu \sim m$ ($\lambda \sim 1/m$). In terms of the renormalization group evolution, the gauge coupling is an irrelevant parameter and the mass is a relevant parameter at this minimum.

In this Letter, we measure the evolution of the coupling constant nonperturbatively on the lattice as the fermion mass is varied. We observe unambiguously the fermion decoupling and the reversal of the coupling constant evolution. The results agree well with the perturbative predictions in background field momentum subtraction (BF-MOM) [22,23] and massive gradient flow [24–26] schemes. Together with the mass spectrum and scaling laws measured in Ref. [30], this gives us a consistent nonperturbative picture of the behavior of the theory from IR to UV scales.

Perturbative renormalization group evolution.—In a mass-dependent renormalization scheme, the evolution of the coupling constant g^2 and the mass m are, in general, determined by a pair of renormalization group (RG) equations,

$$\frac{dg^2}{d\log(\lambda)} = -\beta(g^2, \lambda m), \quad (1a)$$

$$\frac{d\log(m)}{d\log(\lambda)} = \gamma(g^2, \lambda m), \quad (1b)$$

where β and γ in (1) depend on $\lambda m = m/\mu$, i.e., on λ relative to the scale $1/m$ set by the fermion mass. In a

Published by the American Physical Society under the terms of the Creative Commons Attribution 4.0 International license. Further distribution of this work must maintain attribution to the author(s) and the published article's title, journal citation, and DOI. Funded by SCOAP³.

perturbative expansion, the expressions for the mass-dependent β and γ can be written as

$$\beta(g^2, \lambda m) = -2g^2 \sum_{n=0}^{\infty} \beta_n(\lambda m) \left(\frac{g^2}{(4\pi)^2} \right)^{n+1}, \quad (2a)$$

$$\gamma(g^2, \lambda m) = \sum_{n=0}^{\infty} \gamma_n(\lambda m) \left(\frac{g^2}{(4\pi)^2} \right)^{n+1}. \quad (2b)$$

We employ the BF-MOM scheme in the Landau gauge [22]. We use the two-loop result from [23], where the fermion mass dependency in the BF-MOM scheme is implemented in terms of a pole mass [31]. The two-loop running coupling can therefore be determined from the beta function alone, with the first two coefficients given by

$$\beta_0(\lambda m_0) = \frac{11}{3} C_G - \frac{4}{3} T_R N_f b_0(x), \quad (3a)$$

$$\beta_1(\lambda m_0) = \frac{34}{3} C_G^2 - T_R N_f b_1(x), \quad (3b)$$

with $x = -1/(2\lambda m_0)^2$ and m_0 as the fermion pole mass. For SU(2) gauge theory $C_G = 2$ and for fundamental representation fermions $T_R = 1/2$. The expressions for the coefficients $b_0(x)$ and $b_1(x)$ can be found in [23].

In Fig. 1 we illustrate the behavior of the two-loop massive β function as function of the running coupling (top) and the running coupling itself as a function of the length scale (bottom). The evolution curves are obtained by integrating Eq. (1a) numerically (see Supplemental Material [26]) with (3), starting from initial values $(g^2, \lambda) = (g_0^2, \lambda_0)$. As Eq. (1) depends merely on the product of fermion pole mass m_0 and length scale λ , we set $\lambda_0 = 1/(2m_0)$. The different trajectories correspond to different choices of g_0^2 .

We note that the β functions have zeroes at $2\lambda m_0 \approx 1$. These correspond to local minima of the coupling, not to fixed points, because $\beta(g^2, \lambda m_0)$ is vertical here. Our choice of the initial value g_0^2 is very close to the minimum value of the coupling along the evolution curve.

As an example, the evolution curves with $g_0^2 = 1.6$ are highlighted in Fig. 1. For comparison, the figures also show the corresponding asymptotic cases of $N_f = 24$ massless fermions and pure gauge (infinitely heavy and therefore completely decoupled fermions).

Lattice setup.—We simulate a SU(2) gauge theory coupled to $N_f = 24$ mass-degenerate dynamical fermions in the fundamental representation. The corresponding lattice action can be summarized as follows:

$$S = S_G(U) + S_F(V) + c_{\text{SW}} S_{\text{SW}}(V), \quad (4)$$

where U represents SU(2) gauge link matrix in the fundamental representation, V is the corresponding

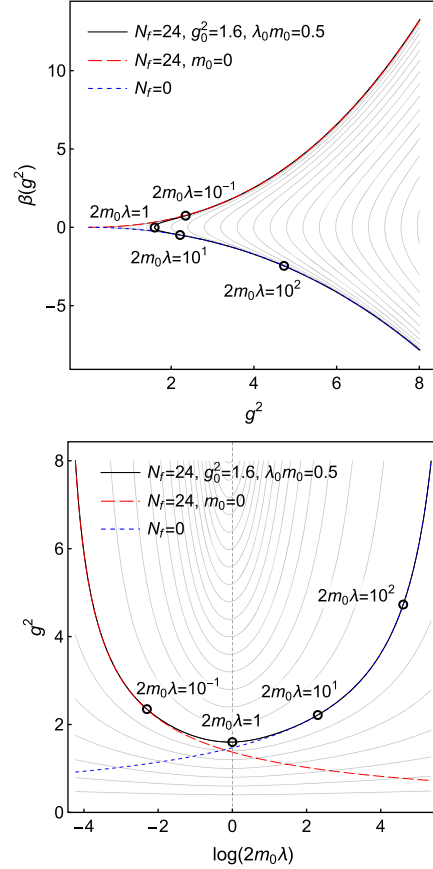


FIG. 1. Top: two-loop β functions for $N_f = 0$ theory (blue, short-dashed) and massless (red, long-dashed) and massive (solid, black) $N_f = 24$ theories. The massive running coupling reaches the minimum value of $g^2 = g_0^2 = 1.6$ at $2m_0\lambda_0 \approx 1$. Bottom: couplings g^2 as functions of the length scale λ , obtained by integrating the β and γ functions. The integration constants have been set to match the asymptotic behavior. In both panels we show the evolution when λ decreases or increases by a factor of 10. The solid gray lines show the curves for the massive $N_f = 24$ theory for different values of g_0^2 . For $g_0^2 > 1.6$, g_0^2 changes by $\Delta g_0^2 = 0.4$ between successive curves, whereas for $g_0^2 < 1.6$, g_0^2 changes by $\Delta g_0^2 = -0.2$.

hypercubically truncated stout smeared link matrix (HEX smearing) [32], S_G is the Wilson gauge action, and S_F and S_{SW} are, respectively, the Wilson fermion action and clover term with Sheikholeslami-Wohlert coefficient $c_{\text{SW}} = 1$ [17].

Simulations are carried out using a hybrid Monte Carlo (HMC) algorithm with leapfrog integrator and chronological initial values for the fermion matrix inversion [33]. The HMC trajectories have unit length and the number of leapfrog steps is set to yield acceptance rates above 80%.

The lattice quark mass is determined via the partially conserved axial-vector current (PCAC) relation

$$a m_q = \left. \frac{(\partial_4^* + \partial_4) f_A(x_4)}{4f_P(x_4)} \right|_{x_4=L/2}, \quad (5)$$

where a is the lattice spacing, ∂_4 and ∂_4^* are forward and backward lattice time-derivative operators, and f_A and f_P are axial and pseudoscalar current correlation functions [34]. Equation (5) receives an $O(a)$ correction, but for smeared quarks it is very small and we omit it here. The bare quark mass from (5) is multiplicatively renormalized; however, the renormalization is expected to vary little as the coupling is changed (see, e.g., [35]), and for our purposes the bare mass is sufficient [26].

We use the running coupling in the nonperturbative gradient flow (GF) scheme [36–38]. In the continuum, it can be written as function of length scale λ as [36]

$$g_{\text{GF}}^2(\lambda) = \frac{2\pi^2\lambda^4\langle E(\lambda)\rangle}{3(N^2-1)}, \quad (6)$$

with $\langle E(\lambda)\rangle$ being the flow-evolved gauge action at flow time $t = \lambda^2/8$. On a lattice of size L^4 with periodic boundary conditions for the gauge field, we use

$$g_{\text{GF}}^2(\lambda_L, L) = \frac{2\pi^2\lambda_L^4\langle E(\lambda_L, L)\rangle}{3(N^2-1)[1 + \delta_{L/a}(\lambda_L/L)]}, \quad (7)$$

as an estimator for Eq. (6), with lattice flow scale λ_L . Here $\langle E(\lambda_L, L)\rangle$ is the expectation value of the clover energy of the flow-evolved lattice gauge field after flow time $t = \lambda_L^2/8$, and

$$\delta_N(c) = \left(\sqrt{\pi}c \sum_{n=-N/2}^{N/2-1} e^{-[Nc \sin(\pi n/N)]^2} \right)^4 - \frac{\pi^2 c^4}{3} - 1 \quad (8)$$

is a finite volume and finite lattice spacing correction for $\langle E(\lambda_L, L)\rangle$. Equation (8) is obtained from the corresponding expression in [39] by replacing continuum with lattice momenta (cf. [40]). The flow is governed by the Lüscher-Weisz action [41].

To relate the GF scheme from Eq. (6) to the BF-MOM scheme from Fig. 1, we make use of the quark-mass-dependent one-loop expression for $\langle E(\lambda)\rangle$ from [24] to derive [25] the leading coefficient of a perturbative expansion of the mass-dependent GF scheme beta function

$$\beta_{0,\text{GF}}(g_{\text{GF}}^2, \lambda m) = \beta_0 + \frac{4}{3} T_R N_f x \frac{d\Omega_{1q}(x)}{dx}, \quad (9)$$

where β_0 is the (universal) leading coefficient of the massless $\overline{\text{MS}}$ scheme, $x = -1/(2m\lambda)^2$, and Ω_{1q} is given in [24], or with our conventions in the Supplemental Material [26]. As the renormalization group equations (1) do not fix the overall scale in either scheme, their respective scales λ_{GF} and λ_{BFM} should be related by a rescaling of the form $\lambda_{\text{GF}} = \rho_s \lambda_{\text{BFM}}$. To determine ρ_s , we require that, for a given quark mass, the behavior of the running coupling near the corresponding decoupling point (where the beta

function changes sign) is as similar as possible [26] in the two schemes. At the one-loop level, this leads to the matching criterion

$$\beta_{0,\text{BFM}}(\lambda_0 m_0) = \beta_{0,\text{GF}}(\lambda_0 m_0 \rho_s), \quad (10)$$

where $\beta_{0,\text{BFM}}$ is the leading BF-MOM beta function coefficient from Eq. (2), and $\lambda_0 = 1/(2m_0)$ is the approximate decoupling scale in the BF-MOM scheme. This yields

$$\rho_s = 2.5359\dots \quad (11)$$

Results.—Most of our analysis is done using ensembles of lattices of size $V = L^4$, $L = 48a$, with smaller lattices used for finite size analysis. These ensembles were used for the spectrum analysis in [30]. The bare lattice gauge coupling is parametrized with $\beta = 4/g_{0,\text{lat}}^2$, and we use values $\beta = 0.25, 0.001$, and -0.25 . Because Wilson fermions induce a positive shift in effective β [42,43], very small and even negative values of β are needed to compensate for this effect with large numbers of fermions. The simulation parameters and the measured PCAC quark masses are listed in Table I.

In Fig. 2 we show examples of $g_{\text{GF}}^2(\lambda_L)$ for $\beta = 0.25, 0.001$ and three different values of m_q , each. The switch from the light quark behavior (left column), where the coupling decreases with distance, to the heavy quark behavior (right column) with increasing coupling is evident. We compare with the two-loop perturbation theory by fitting g_0^2 and $\lambda_0 m_0$ to match g_{GF}^2 . In effect, the fit procedure achieves the relative multiplicative renormalization between λm_0 in BF-MOM scheme and $\lambda_L m_q$ on the lattice.

For concreteness, we set $\lambda_0 = a$ so that $\lambda = \lambda_L$ and determine the pair (g_0^2, m_0^2) corresponding to a given pair (β, m_q) by a least-squares fit. The fit is carried out over the range $\lambda_L/a \in [4.8, 20]$. Thus, on a given lattice, we are able to follow the evolution of the coupling over a scale factor of 4. The fit between the lattice data and the perturbative coupling is, in general, very good, well within the statistical error of each g_{GF}^2 curve, with the exception of the largest couplings $g_{\text{GF}}^2 \gtrsim 10$. The fit parameters are listed in Table I.

We have checked the finite volume effects by analyzing g_{GF}^2 on lattices with $L/a = 32, 40$, and 48 . The volume dependence is small and for $\lambda_L/L \in [0.1, 0.4]$ within the statistical errors; an example of this is shown in Fig. 3. Thus, we do the final analysis using only the largest volume results.

From Table I we can observe that $am_q r_s \sim \lambda_0 m_0$ with $r_s \approx 0.4\text{--}0.5$ in all cases where the fit is reliable (at very small m_q the fit becomes compatible with a vanishing quark mass). This suggests that the relative scale renormalization between the lattice and the BF-MOM scheme is approximately constant in the studied range and the rescaling factor $r_s = 1/\rho_s$ can be considered compatible with Eq. (11) with the given systematic uncertainties.

TABLE I. Simulation parameters, PCAC quark mass, fitted g_0^2 and m_0 (where fit was possible), ratio $r_s = \lambda_0 m_0 / (am_q)$, HMC acceptance (Acc.), and the total number of gauge configurations used in the analysis. The indicated uncertainties are statistical (Stat.) ones.

β	κ	am_q	g_0^2	$\lambda_0 m_0$	r_s	Acc.	Stat.
-0.25	0.1309	0.0202(1)	1.783(2)	0.010(1)	0.50	0.91	1.3×10^3
-0.25	0.129	0.1001(1)	2.002(4)	0.052(1)	0.52	0.91	2.9×10^3
-0.25	0.1277	0.1608(1)	2.192(6)	0.083(1)	0.52	0.9	3.0×10^3
-0.25	0.1263	0.2266(1)	2.47(2)	0.111(2)	0.49	0.91	3.2×10^3
-0.25	0.125	0.3013(2)	2.74(3)	0.156(3)	0.52	0.91	3.3×10^3
-0.25	0.123	0.4546(3)	4.05(4)	0.203(3)	0.45	0.91	3.5×10^3
0.001	0.1299	0.0170(1)	1.664(2)	0.016(1)	0.94	0.92	2.1×10^3
0.001	0.129	0.0517(1)	1.760(2)	0.022(1)	0.43	0.93	1.3×10^3
0.001	0.125	0.2179(1)	2.191(6)	0.105(1)	0.48	0.92	3.2×10^3
0.001	0.12	0.5074(3)	3.44(5)	0.239(5)	0.47	0.93	3.6×10^3
0.25	0.129	0.0151(1)	1.573(2)	0.011(1)	0.73	0.91	1.9×10^3
0.25	0.125	0.1658(1)	1.929(5)	0.068(1)	0.41	0.93	2.9×10^3
0.25	0.12	0.3853(1)	2.49(2)	0.170(3)	0.44	0.93	3.6×10^3
0.25	0.115	0.7534(7)	0.94	3.4×10^3

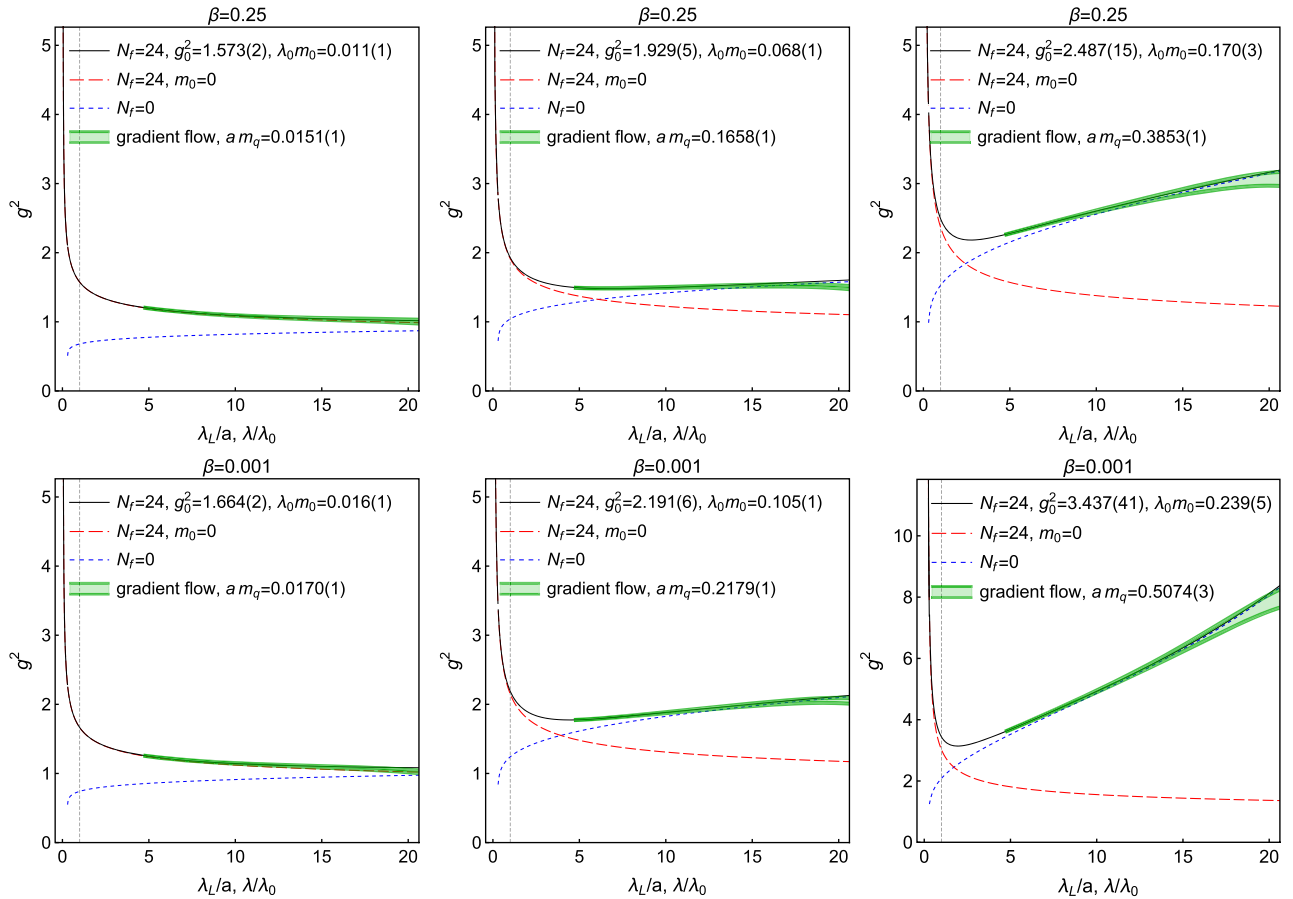


FIG. 2. The measured gradient flow running coupling (green bands), obtained on a $V = (48a)^4$ lattice at $\beta \in \{0.25, 0.001\}$ at three quark masses m_q , to which two-loop running coupling is fitted (solid black line). The gradient flow length scale λ_L is shown in interval $\lambda_L/a \in [4.8, 20]$. In comparison, the matched pure gauge SU(2) (blue dotted line) and $N_f = 24$, $m_q = 0$ (red dashed line) couplings are also shown.

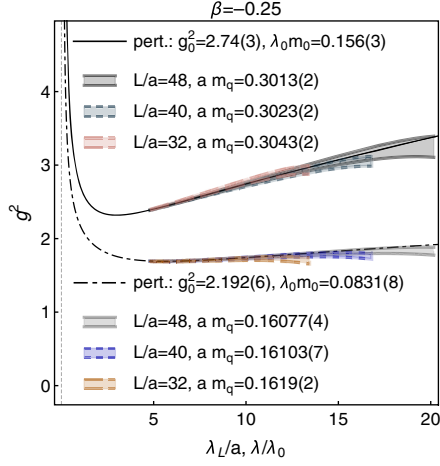


FIG. 3. g_{GF}^2 measured from $L = 32a, 40a$, and $48a$ lattices at $\beta = -0.25$, $\kappa = 0.125$ ($am_q \approx 0.30$), respectively, $\kappa = 0.1277$ ($am_q \approx 0.16$), together with corresponding perturbative curves (pert.). The flow is plotted in the interval $4.8a < \lambda_L < 0.42L$.

In Fig. 4 we plot all measurements of g_{GF}^2 against $2m_q\lambda_L/\rho_s$, with ρ_s from Eq. (11), overlaid with the perturbative g^2 from Fig. 1. There are no fitted parameters. The lattice data follow the two-loop perturbative curves remarkably well, independent of the value of β . We have verified that the two-loop BF-MOM running coupling should be a good approximation to the perturbative massive RG running coupling [26]. There are cases where simulation results with different β and m_q fall on curves that are very close to each other. Since different values of β and m_q imply, in general, different lattice spacings, this

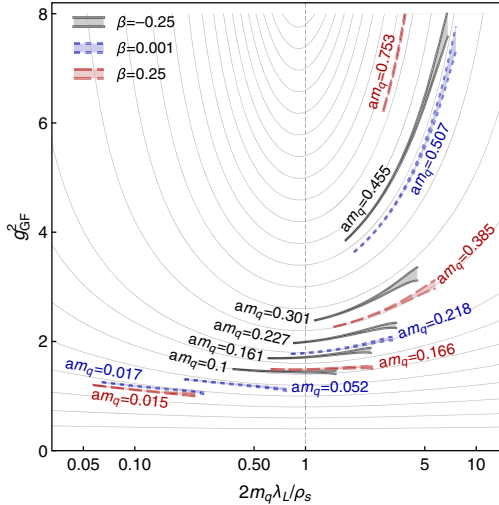


FIG. 4. The lattice gradient flow running coupling (black, blue, and red error bands) as function of $2m_q\lambda_L/\rho_s$, where m_q is the PCAC quark mass and ρ_s is given by Eq. (11). The data are superimposed to the massive two-loop gradient flow curves from the lower panel of Fig. 1.

demonstrates that the results scale when the lattice spacing is varied. In contrast to the asymptotically-free lattice QCD, the lattice spacing becomes smaller when β is decreased, and the theory does not have a continuum limit because of the UV Landau pole.

Conclusions.—Using SU(2) gauge theory with $N_f = 24$ fermions of mass m , we have presented a clear non-perturbative demonstration of the decoupling of fermions at distance scale $\sim 1/m$. At the same time, the behavior of the theory changes dramatically: at smaller distances, the theory behaves as IR trivial, nonasymptotically-free theory, with coupling decreasing with distance, whereas at longer distances it behaves like pure gauge SU(2) theory with increasing coupling. Together with the study of the excitation spectrum in this theory [30], this provides a consistent nonperturbative description of the behavior of the theory from IR to UV scales.

The support of the Academy of Finland Grants No. 308791, No. 310130, and No. 320123 is acknowledged. Partially funded by the Swiss National Science Foundation (SNSF) through Grant No. 200021_175761. The authors wish to acknowledge CSC—IT Center for Science, Finland, for generous computational resources.

* trindlis@itp.unibe.ch

† kari.rummukainen@helsinki.fi

‡ ahmed.salami@helsinki.fi

§ kimmo.i.tuominen@helsinki.fi

- [1] F. Sannino and K. Tuominen, Orientifold theory dynamics and symmetry breaking, *Phys. Rev. D* **71**, 051901 (2005).
- [2] C. T. Hill and E. H. Simmons, Strong dynamics and electroweak symmetry breaking, *Phys. Rep.* **381**, 235 (2003); **390**, 553(E) (2004).
- [3] D. D. Dietrich, F. Sannino, and K. Tuominen, Light composite Higgs from higher representations versus electroweak precision measurements: Predictions for CERN LHC, *Phys. Rev. D* **72**, 055001 (2005).
- [4] A. Arbey, G. Cacciapaglia, H. Cai, A. Deandrea, S. Le Corre, and F. Sannino, Fundamental composite electroweak dynamics: Status at the LHC, *Phys. Rev. D* **95**, 015028 (2017).
- [5] T. Karavirta, J. Rantaharju, K. Rummukainen, and K. Tuominen, Determining the conformal window: SU(2) gauge theory with $N_f = 4, 6$ and 10 fermion flavours, *J. High Energy Phys.* **05** (2012) 003.
- [6] V. Leino, J. Rantaharju, T. Rantalaiho, K. Rummukainen, J. M. Suorsa, and K. Tuominen, The gradient flow running coupling in SU(2) gauge theory with $N_f = 8$ fundamental flavors, *Phys. Rev. D* **95**, 114516 (2017).
- [7] V. Leino, K. Rummukainen, J. M. Suorsa, K. Tuominen, and S. Tähtinen, Infrared fixed point of SU(2) gauge theory with six flavors, *Phys. Rev. D* **97**, 114501 (2018).
- [8] V. Leino, K. Rummukainen, and K. Tuominen, Slope of the beta function at the fixed point of SU(2) gauge theory with six or eight flavors, *Phys. Rev. D* **98**, 054503 (2018).

- [9] A. Amato, V. Leino, K. Rummukainen, K. Tuominen, and S. Tähtinen, From chiral symmetry breaking to conformality in SU(2) gauge theory, [arXiv:1806.07154](https://arxiv.org/abs/1806.07154).
- [10] A. J. Hietanen, J. Rantaharju, K. Rummukainen, and K. Tuominen, Spectrum of SU(2) lattice gauge theory with two adjoint Dirac flavours, *J. High Energy Phys.* **05** (2009) 025.
- [11] A. J. Hietanen, K. Rummukainen, and K. Tuominen, Evolution of the coupling constant in SU(2) lattice gauge theory with two adjoint fermions, *Phys. Rev. D* **80**, 094504 (2009).
- [12] L. Del Debbio, A. Patella, and C. Pica, Higher representations on the lattice: Numerical simulations. SU(2) with adjoint fermions, *Phys. Rev. D* **81**, 094503 (2010).
- [13] L. Del Debbio, B. Lucini, A. Patella, C. Pica, and A. Rago, Conformal versus confining scenario in SU(2) with adjoint fermions, *Phys. Rev. D* **80**, 074507 (2009).
- [14] L. Del Debbio, B. Lucini, A. Patella, C. Pica, and A. Rago, Mesonic spectroscopy of minimal walking technicolor, *Phys. Rev. D* **82**, 014509 (2010).
- [15] F. Bursa, L. Del Debbio, D. Henty, E. Kerrane, B. Lucini, A. Patella, C. Pica, T. Pickup, and A. Rago, Improved lattice spectroscopy of minimal walking technicolor, *Phys. Rev. D* **84**, 034506 (2011).
- [16] T. DeGrand, Y. Shamir, and B. Svetitsky, Infrared fixed point in SU(2) gauge theory with adjoint fermions, *Phys. Rev. D* **83**, 074507 (2011).
- [17] J. Rantaharju, T. Rantalaiho, K. Rummukainen, and K. Tuominen, Running coupling in SU(2) gauge theory with two adjoint fermions, *Phys. Rev. D* **93**, 094509 (2016).
- [18] L. Del Debbio, B. Lucini, A. Patella, C. Pica, and A. Rago, Large volumes and spectroscopy of walking theories, *Phys. Rev. D* **93**, 054505 (2016).
- [19] D. J. Gross and F. Wilczek, Ultraviolet Behavior of Non-Abelian Gauge Theories, *Phys. Rev. Lett.* **30**, 1343 (1973).
- [20] H. D. Politzer, Reliable Perturbative Results for Strong Interactions?, *Phys. Rev. Lett.* **30**, 1346 (1973).
- [21] V. Leino, T. Rindlisbacher, K. Rummukainen, K. Tuominen, and F. Sannino, Safety versus triviality on the lattice, *Phys. Rev. D* **101**, 074508 (2020).
- [22] A. Rebhan, Momentum subtraction scheme and the background field method in QCD, *Z. Phys. C* **30**, 309 (1986).
- [23] F. Jegerlehner and O. V. Tarasov, Exact mass dependent two loop anti-alpha(s)(Q²) in the background MOM renormalization scheme, *Nucl. Phys.* **B549**, 481 (1999).
- [24] R. V. Harlander and T. Neumann, The perturbative QCD gradient flow to three loops, *J. High Energy Phys.* **06** (2016) 161.
- [25] R. V. Harlander, The gradient flow at higher orders in perturbation theory, *Proc. Sci., LATTICE2021* (2022) 489 [[arXiv:2111.14376](https://arxiv.org/abs/2111.14376)].
- [26] See Supplemental Material at <http://link.aps.org/supplemental/10.1103/PhysRevLett.129.131601> for details on (1) the numerical method to integrate the RG equations, (2) the method to obtain the gradient flow beta function, (3) the method to match the gradient flow and the BF-MOM scheme, (4) a comparison of the one- and two-loop perturbative running couplings, and (5) possible effects from three-loop nonuniversality in the massless and pure gauge limit, which includes Refs. [27–29].
- [27] S. Sint and Peter Weisz (ALPHA Collaboration), The running quark mass in the SF scheme and its two loop anomalous dimension, *Nucl. Phys.* **B545**, 529 (1999).
- [28] M. Dalla Brida and A. Ramos, The gradient flow coupling at high-energy and the scale of SU(3) Yang–Mills theory, *Eur. Phys. J. C* **79**, 720 (2019).
- [29] S. A. Larin and J. A. M. Vermaseren, The three loop QCD Beta function and anomalous dimensions, *Phys. Lett. B* **303**, 334 (1993).
- [30] J. Rantaharju, T. Rindlisbacher, K. Rummukainen, A. Salami, and K. Tuominen, Spectrum of SU(2) gauge theory at large number of flavors, *Phys. Rev. D* **104**, 114504 (2021).
- [31] K. Hagiwara and T. Yoshino, On the gauge dependence of the renormalization group function in quantum chromodynamics, *Phys. Rev. D* **26**, 2038 (1982).
- [32] S. Capitani, S. Durr, and C. Hoelbling, Rationale for UV-filtered clover fermions, *J. High Energy Phys.* **11** (2006) 028.
- [33] R. C. Brower, T. Ivanenko, A. R. Levi, and K. N. Orginos, Chronological inversion method for the Dirac matrix in hybrid Monte Carlo, *Nucl. Phys.* **B484**, 353 (1997).
- [34] M. Lüscher, S. Sint, R. Sommer, P. Weisz, and U. Wolff, Nonperturbative $O(a)$ improvement of lattice QCD, *Nucl. Phys.* **B491**, 323 (1997).
- [35] I. Campos, P. Fritzsche, C. Pena, D. Preti, A. Ramos, and A. Vladikas (ALPHA Collaboration), Non-perturbative quark mass renormalisation and running in $N_f = 3$ QCD, *Eur. Phys. J. C* **78**, 387 (2018).
- [36] M. Lüscher, Properties and uses of the Wilson flow in lattice QCD, *J. High Energy Phys.* **08** (2010) 071; **03** (2014) 092(E).
- [37] Z. Fodor, K. Holland, J. Kuti, D. Negradi, and C. H. Wong, A new method for the beta function in the chiral symmetry broken phase, *EPJ Web Conf.* **175**, 08027 (2018).
- [38] C. T. Peterson, A. Hasenfratz, J. van Sickle, and O. Witzel, Determination of the continuous β function of SU(3) Yang-Mills theory, *Proc. Sci., LATTICE2021* (2022) 174 [[arXiv:2109.09720](https://arxiv.org/abs/2109.09720)].
- [39] Z. Fodor, K. Holland, J. Kuti, D. Negradi, and C. H. Wong, The Yang-Mills gradient flow in finite volume, *J. High Energy Phys.* **11** (2012) 007.
- [40] P. Fritzsche and A. Ramos, The gradient flow coupling in the Schrödinger functional, *J. High Energy Phys.* **10** (2013) 008.
- [41] M. Lüscher and P. Weisz, On-shell improved lattice gauge theories, *Commun. Math. Phys.* **97**, 59 (1985); **98**, 433(E) (1985).
- [42] A. Hasenfratz and T. A. DeGrand, Heavy dynamical fermions in lattice QCD, *Phys. Rev. D* **49**, 466 (1994).
- [43] T. Blum, C. E. DeTar, U. M. Heller, L. Karkkainen, K. Rummukainen, and D. Toussaint, Thermal phase transition in mixed action SU(3) lattice gauge theory and Wilson fermion thermodynamics, *Nucl. Phys.* **B442**, 301 (1995).